博士論文（要約）

Development of photoactivatable heterotrimeric G-proteins and an affibody-based engineered system to switch cellular processes

（光駆動型ヘテロ三量体 G タンパク質及び Affibody に基づく細胞操作技術の開発）

俞　改改

Development of photoactivatable heterotrimeric G-proteins and an affibody-based engineered system to switch cellular processes

by

Gaigai YU

Thesis submitted to The University of Tokyo
For the Degree of Doctor of Arts and Science

Department of General Systems Studies,
Graduate School of Arts and Sciences,
The University of Tokyo

Abstract

Techniques for manipulating biological phenomena with light have been developed greatly in recent years. However, the optical manipulation of heterotrimeric G proteins, which cover the activation of diverse types of plasma membrane receptor to a variety of intracellular processes, has not been achieved. In Chapter 2 of the present study, I demonstrated an optogenetic method using photoswitchable dimerization systems to manipulate the heterotrimeric G proteins. I succeeded in induction of two typical second messengers: Ca^{2+} and cAMP in mammalian cells, by the optical manipulation of $G\alpha_q$ and $G\alpha_s$ with multicolor. Because light has superior temporal and spatial resolution, the development of this optical approach achieves the regulation of the second messengers with high spatiotemporal resolution.

In Chapter 3 of this study, I developed a new system to manipulate protein of interest (POI) in mammalian cells, which I named the affibody-based TI-DrBphP system. This system allows for simultaneous manipulation of two POIs with single stimulus, which is not generally practicable by existing technologies. Engineering of the chemically activatable TEV (CA-TEV), the temperature sensitive TEV and the photoactivatable TEV (PA-TEV), making it possible to actuate this system by rapamycin, temperature or light stimuli. Furthermore, the case study on a key molecule of necrosis, the MLKL protein in the TI-DrBphP system demonstrated that cellular death signaling was switchable by rapamycin induction. The technology provided in this study will expand the application of translocation-based approaches, because simultaneous regulation of different POIs, which is difficult with conventional techniques, can be simply achieved taking advantage of the affibody-based TI-DrBphP system.

Table of contents

Chapter 1: General introduction

1-1. Optogenetics

Optogenetics[1] is the biological technique that uses a combination of optical and genetic method to manipulate the function of well-defined biochemical events in specific cells or living tissues. The history of optogenetics traced back to the year 1971, Stoeckenius and Oesterhelt discovered that bacteriorhodopsin acts as an ion pump that can be rapidly activated by visible-light photons[2], and in the year 1975, halorhodopsin was identified by Matsuno and Mukohata[3]. The widely known modern optogenetics started since 2002, when channelrhodopsin was firstly reported by Hegemann and co-workers[4]. A breakthrough of optogenetics occurred in the year 2005, Boyden and co-workers made cells light sensitive using only a single construct. They described that upon introduction of a microbial opsin gene without any other parts, chemicals or components, neurons became precisely responsive to light[5]. Optogenetics grew significantly in the years after 2005, a number of additional researches were consecutively reported and by the year of 2010, all of bacteriorhodopsin, halorhodopsin and channelrhodopsin had been proved capable of turning neurons on or off, rapidly and safely, in response to diverse colors of light [6-8].

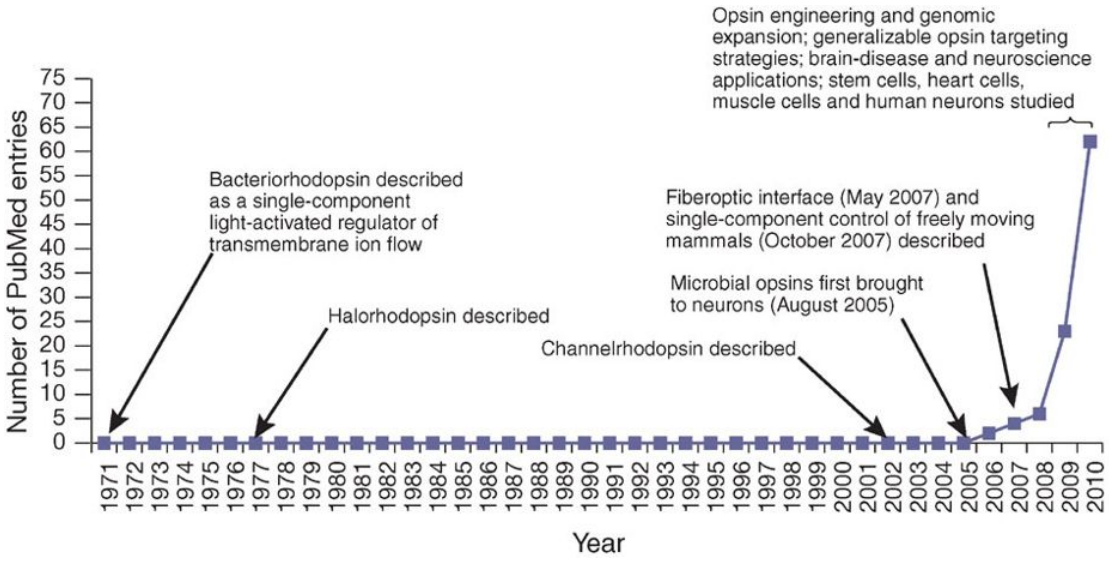

Figure 1-1. History of optogenetics[9].

Because optogenetics allows the possibility to identify particular neurons and networks, this technique was typically used to control neurons in the early stage of researches. For example, by using of the optogenetic actuator channerlrhodopsin, it

has been succeed to drive activation of non-excitable glial cells[10].

Molecule evolution has successfully enabled optogenetics to manipulate wide range of biochemical events[11, 12, 13]. The classic example is the use of optogenetic tool to temporal control of signals by the photosensitive proteins utilized in various cell signaling pathways. More specifically, Arian and co-workers described optical control of distinct G protein-coupled receptor (GPCR) biochemical pathways in freely moving mammals using vertebrate rhodopsin-GPCR chimeras (optoXRs)[11], which recruit pathways that are governed by distinct heterotrimeric G-protein pathways.

The latest development of photoswitch proteins also played an essential role in the advancement of optogenetics. It further extended the optogenetics to allow light control of various functional proteins, such as CRISPR associated protein 9 (Cas9)[14], which is an RNA-guided DNA endonuclease enzyme, and Cre recombinase[15], which is an enzyme that catalyzes recombination between two lox-P sites. Photoactivatable activatable CRISP-Cas9[16] has allowed for using light to control genome editing. Photoactivatable Cre-loxP recombination system[17], allows for efficient DNA recombination so as to achieve optogenetic genome engineering. These approaches provide convenient and precise way for optogenetic manipulate diverse cellular processes in vitro and in vivo.

Since channelrhodopsin was first used to control the activity of mammalian neurons in 2005, a great deal of progress has been made in a short period of time. It is undoubtedly that optogenetics will constantly contribute to various fields of scientific researches in future.

1-2. Second messengers and heterotrimeric G proteins

Second messengers are important molecules as the intracellular signaling substance. For example, Ca^{2+}, one of the second messengers, supports various life activities such as muscle contraction and inflammation. In addition, it is known that cAMP, another second messenger controls biological processes such as lipolysis through activation of protein kinase, and also plays a major role in memory in the brain. Complex signaling works in the cell, one of which is signaling by G protein-coupled receptor (GPCR). GPCR-bound G proteins catalyze guanine nucleotide exchange on the α subunit of heterotrimeric G proteins (Gα)[18]. Gα activates effector proteins such as phospholipase and adenylyl cyclase, which modulates the second messengers including Ca^{2+} and cAMP. When the extracellular signaling substance binds to the G protein-coupled receptor, the Gα is activated[19]. It then activates the corresponding effector protein by approaching and interacting with it. Next, the effector protein produces second messenger and so as to regulate the cell function (Figure 1-2).

G-protein α subunit

Gα	effector	second messenger
$G\alpha_q$	Phospholipase C Beta (Plcβ)	increase IP_3, Ca^{2+}
$G\alpha_s$	Adenylate Cyclase (AC)	increase cyclic AMP (cAMP)

Figure 1-2. Typical Gα and the corresponding effector. Activation of the Gα modulates the release of second messengers.

1-3. Conventional methods to manipulate G proteins

Chemically-inducible dimerization (CID) system: FKBP/FRB[20], has been applied to achieve precise manipulation of Gα previously[21, 22]. Specifically, Putyrski and Schultz developed a method based on rapamycin-dependent system to bypass the GPCR by direct activation of Gα, which induces downstream signaling cascades. They demonstrated the plasma membrane recruitment of constitutively active form of $G\alpha_q$ and $G\alpha_s$ results in the activation of their corresponding effectors. However, it was reported that rapamycin was hardly removed from the FKBP/FRB by washing treatment[23]. Despite the achievement gained through the robust protein-protein interaction using CID system, the drawback is that it hardly reaches spatiotemporal control because of the diffusiveness of chemical cofactor and the irreversibility of the chemical dimerization.

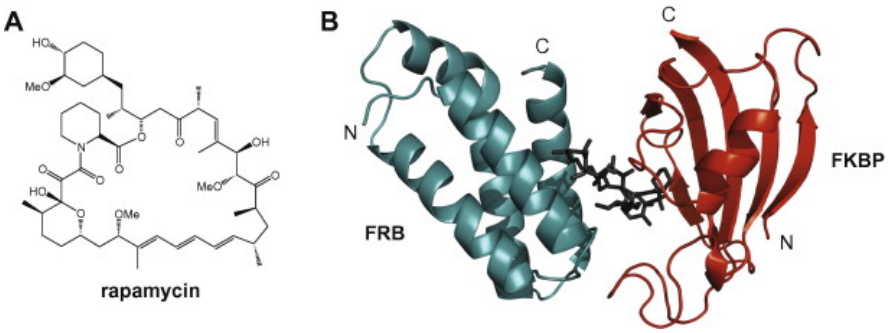

Figure1-3. Chemically inducible dimerization system: FKBP/FRB. This system has been widely used for rapamycin-inducible heterodimerization of fusion proteins.

On the other hand, optogenetic tools like optoXRs, which allow achieving high spatiotemporal precision, have been developed for manipulation of Gα. OptoXRs are composed of an extracellular component derived from light sensitive rhodopsin and an intercellular component derived from GPCR. In spite of optoXRs allowing the optogenetic control of intracellular signal transduction, a limitation of it is that rhodopsin gets broad absorption band. Practically, fluorescent tools (e.g. GCaMP[24, 25, 26]) used as biomarkers or biosensors are commonly required to evaluate the effect of the optogenetic perturbation on the cell. However, optoXRs are usually incompatible with these tools because the excitation wavelength of the fluorescent tools may potentially perturb the function of optoXRs having broad absorption band.

1-4. Photoswitches

Photoswitches are photoswitchable dimerization proteins that sensitive to light, their interactions can be controlled using different light stimulation. These proteins are powerful tools that can be used to optogenetically manipulate molecular processes in biological systems. Most light-induced protein-protein interactions are dependent on blue light, for example, AsLOV2[27], iLID system[28], CRY2-CIB1 system[29] and Magnet system[30]. AsLOV2 is a light-sensitive protein developed from the Light, oxygen, or voltage (LOV) domain of Avena Sativa phototropin 1[31], which is a class of photoreceptor proteins sensitive to blue light through a noncovalently bound flavin chromophore. Because of the large conformation change in the α-helical region (Jα) of AsLOV2 upon blue light irradiation (Figure 1-4), it can be used to photomodulate the affinity of peptides for binding partners, such as the SsrA peptide[32], which binds to SspB and shares sequence identity with the Jα of AsLOV2. Through the engineering of the SsrA peptide against the AsLOV2 domain, Gurkan and his colleagues developed the improved light-induced dimer (iLID) system. They characterized two different photoswitches according to the different binding affinities of the heterdimerizations, called iLID nano (makes use of wild-type SspB) and iLID micro (makes use of SspB R73Q), respectively.

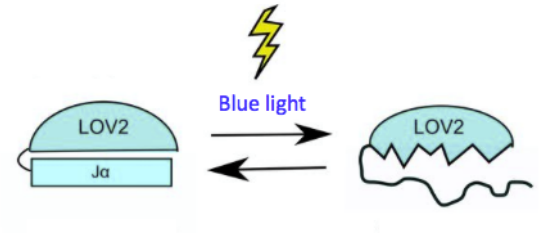

Figure 1-4. Conformation change of Jα in AsLOV2 upon light irradiation.

In addition, light-dependent protein-protein interaction between cryptochrome 2 (CRY2) and cryptochrome-interacting basic-helix-loop-helix protein (CIB1) was identified by Liu and his colleagues. CIB1 interacts with CRY2 in a blue light-specific manner. Magnet system, which is engineered from the fungal photoreceptor Vivid[33], a small light-oxygen-voltage (LOV) domain-containing protein. The original

homodimerization of Vivid was engineering to generate blue light-induced heterodimerization between nMag and pMag through electrostatic interactions.

Except the blue light dependent photoswitches, red and far-red (near-infrared) photoswitches have also been developed. Arabidopsis thaliana phytochrome B (PhyB) and its binding partner, PhyB interaction factors (PIFs) [34-38], which is a photoswitch engineered from photoreceptor in plants has been achieved the light-induced heterodimerization with near-infrared light. It is noteworthy that phytochromobilin (PϕB) or phycocyanobilin (PCB), which serve as the chromophore for PhyB, should be added to PhyB/PIF6 system to support its photosensitivity in mammalian cells. Besides, *Rhodopseudomonas palustris* BphP1 (RpBphP1)[39] and its binding partner PpsR2 was recently reported by the researchers in Verkhusha's group[40], which could be used to activate cellular functions such as transcription by near-infrared light, and to reverse these functions by red light or darkness. However, the big size and oligomeric behavior of PpsR2 limits its application as optogenetic tools. To address this problem, a down-sized binder of RpBphP1: Q-PAS1 has also been developed from the same research group[41]. Q-PAS1 is three-fold smaller than PpsR2 and lacks oligomerization. The superiority of Q-PAS1 makes it more convenient than the natural binding partner PpsR2.

Two different photoswitches: blue light activatable Magnet system and red light activatable PhyB/PIF6 system were used in this study. In Magnet system, the dimerization between nMag and pMag can be induced with blue light. In PhyB/PIF6 system, the interaction and dissociation can be reversibly controlled with red light and far-red light (Figure 1-5). Application of these photoswitches makes it possible to regulate various cellular processes involved in signal transduction by multi-color.

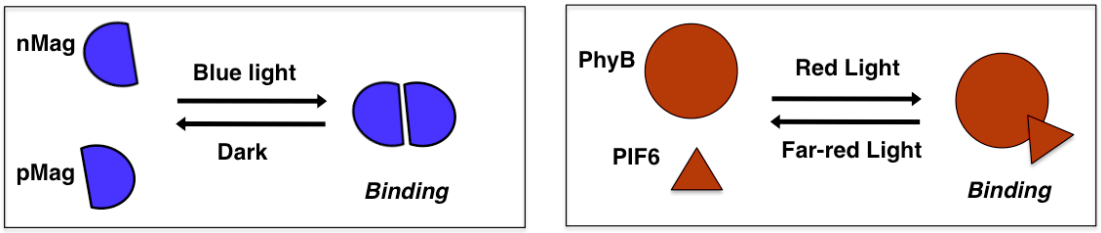

Figure 1-5. Photoswitchable dimerization proteins. (Left) Magnet system; (Right) PhyB/PIF6 system.

1-5. Molecular evolution

Molecular evolution of the photoreceptor protein is required for the development of photoswitches. Various kinds of methods such as phage display[42], yeast display[43], mRNA display[44] and ribosome display[45] were developed and applied in the field of molecular evolution. These display techniques offer powerful discovery in protein engineering. For example, phage display screening was used in the development of the iLID system from the original light-inducible dimer (oLID)[46], which did not have large changes in binding affinity with blue light stimulation. In order to find mutations throughout the Jα-helix domain which stabilize its docked state in dark. The authors created a directed library based on the Rosetta's pmut_scan[47] and fused this library to the phage III coat protein and an N-terminal twin-arginine translocation secretion sequence for display on the surface of phage[48]. After several rounds of phage display selection, phages represented hottest candidates of phenotype were collected, and their genotype were re-cloned and further analyzed by ELISA[49]. Through the screening of recombined point mutants using of high-throughput phage display technology, they succeed in improving the dynamic range of oLID to get iLID by greatly reducing the dark state binding.

Another case is that in the development of LOV2 trap and release of protein (LOVTRAP)[50], mRNA display screening was used. LOVTRAP is an optogenetic approach for reversible light-induced protein dissociation. The Authors generated a mRNA-protein fusion library using a scaffold derived from the Z domain of immunoglobulin-binding staphylococcal protein A[51], which contains about 5×10^{13} unique variants. When the panning against target protein LOV was finished, the bound mRNA–protein was eluted and reverse transcription was performed to convert the mRNA–protein into cDNA/mRNA. The enriched cDNA library was regenerated by PCR for the next round selection. In order to find a protein only bind to the dark state of LOV2, they intelligently took advantage of two previously reported mutants in LOV2: mutant fixed in the dark state-C450A[52] and a light state mutant-I539E[53] in the process of screening strategy. Specifically, in rounds 1-5, the selected library was washed with washing buffer and eluted by incubating with eluting buffer, while in rounds 6-12 the selected library was were washed with washing buffer containing

LOV2 (I539E) to minimize the enrichment of sequences that bound to the light form of LOV2, and competitively eluted by incubating with buffer containing LOV2 (C450A). After a total 12 rounds of selection, they picked up 120 colonies for sequencing from the enriched cDNA library, and they succeed in separating three different Zdk variants, which binding to the target protein LOV with high affinities in dark state but weak affinities in light state.

Each technology has its own varying drawbacks. For example the slow growth rates of phage limit screening to one round of for several days, while in the yeast-based cell secretion and capture technologies, secreted binding proteins are not captured until after they have completely left the cell, leading to a potential loss of the genotype-phenotype linkage. In this study, I performed in vitro protein evolution using the ribosome display technology to create new proteins that can be bind to the desired target protein. Comparing to the other display methods, a main advantage of ribosome display is the big library size (~10^{13}), and the diversity of the library is not limited by the transformation efficiency of bacterial cells, but only by the number of ribosomes and different mRNA molecules present in the test tube. Except to this, the screening process for every round in ribosome display is faster because the in vitro translation of cDNA library to generate protein library is quick, which is not limited by the slow growth rates of bacterial cells.

The display technologies offer possibility to get new candidate binding partner of target proteins. However, these methods only provide the enriched proteins as the output, the detailed DNA sequences coupled to the enriched proteins is still not clear. In order to efficiently analyze the DNA sequences, I considered the technology of next-generation sequencing (NGS)[54, 55]. NGS is able to provide millions of sequences of libraries or defined selection cycles within a very short time. This allows for the first time an unprecedented deep insight into the evolutionary processes within an individual biopanning.

1-6. Scaffold proteins

Scaffold proteins always play important roles in molecular evolution. Because not only they can be used to generate protein library to create new genetically encodable binders of target proteins, but also short peptides with known affinity against a target can be inserted into a scaffold for protein engineering. Various scaffolds, such as nanobody[56], monobody[57] and the designed ankyrin repeat proteins (DARPins)[58] have been developed to enable protein function to be regulated (Figure1-6).

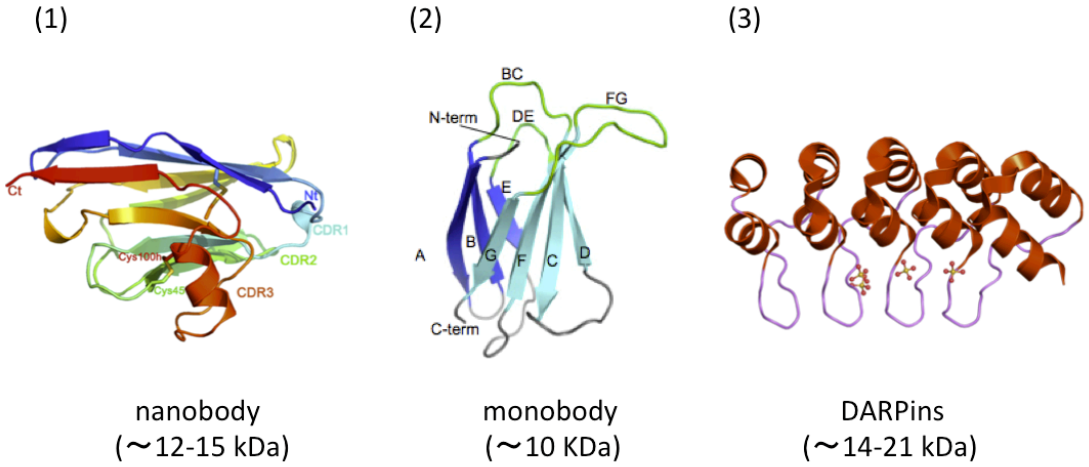

Figure 1-6. Crystal structures of different scaffold proteins.

However, the disulfide bond formation between cysteine and cysteine residues make the nanobody unstable in reducing environment of a cell. The big size of DARPins limits its application in different display technologies. Monobody is an attractive scaffold protein, but the numerous randomization positions in three loops make it relatively complicated to construct the corresponding DNA library. Owning to this reason, monobody becomes a second choice for us. In this study, we focused on the potential and advantages of another protein called affibody[59]. Affibody is a member of the family of antibody mimetics, the original affibody protein was designed based on the Z domain (the immunoglobulin G binding domain) of protein A. It is a useful scaffold to create protein library used in the screening system, for the purpose to find new binding partners of target proteins. Affibodies are small (~7 kDa) but robust proteins that engineered to a large number of target proteins with high affinity[60, 61, 62]. Similar to the antibody which is composed of the constant region and the variable

region, the structure of affibody consists of three helixes, and 13 amino acids in helix 1 and helix 2 (red 'X' highlighted in Figure 1-7) are available to randomize without destroying the structure. In this study, DNA library was constructed to get affibody molecules, which containing the NNK codon in the 13 randomization positions of the scaffold, and this library was used in ribosome display to screen binding candidates of the target protein: DrBphP-PSM[63].

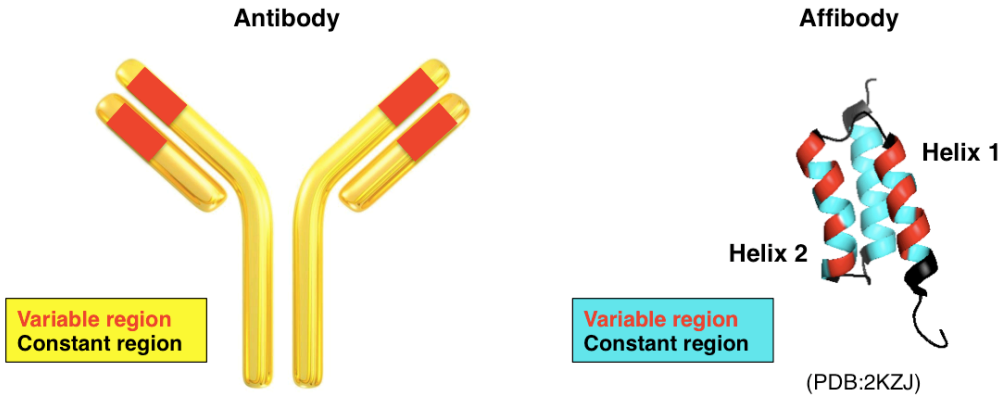

Figure 1-7. Crystal structure and sequence information of affibody, a member of the family of antibody mimetics. The randomization positions in affibody scaffold are highlighted in red.

1-7. Purpose of the present study

Techniques for manipulating biological phenomena by light have been developed in recent years. However, the light manipulation of heterotrimeric G proteins, one of the most important proteins modulating signal molecules in mammalian cells, has not been achieved. In order to control the heterotrimeric G proteins with light, we focused on approaches to photoactive proteins, which called optical approaches[64]. Optical approaches offer optical control of target proteins so as to manipulate their function. The purpose of this study in Chapter 2 is to develop photoactivable heterotrimeric G proteins. By the combination of photoswitches and the α subunit of heterotrimeric G proteins (Gα), it is capable to manipulate the subcellular localization of Gα through light illumination so as to optically induce the second messengers in mammalian cells. Because light has high spatiotemporal resolution, the development of this approach will achieve the control of the second messengers with superior spatiotemporal resolution, offering greater convenience than the existing approaches.

Another research purpose of this study is to make progress in development of new technology to manipulate cellular processes through protein engineering. Despite existing biological approaches, including the optical approaches, offer precise control of target proteins so as to regulate the biological response, they are limited because they are merely available to control single protein of interest (POI). For example, by the usage of two different photoswitches, it is possible to manipulate protein A with blue light and protein B with red light, respectively. However, it is impossible to control these two proteins simultaneously by monochromatic light. Sometimes, integration of different POIs is indispensable to comprehensively explain complex biological phenomena. In order to meet such demands faced in future researches, a system that can simultaneously manipulate multiple POIs is required. In Chapter 3, we sought to engineer a new system, named affibody-based TI-DrBphP system, which enables the simultaneous control of two different proteins. The system can be granted functions by fusing it to various functional proteins to achieve the goal of directly visualizing or regulating target proteins in living cells. With the development of this system, it will become possible to obtain insights into more complicated biological phenomena, which could not be achieved by conventional techniques.

Chapter 2: Optical manipulation of heterotrimeric G proteins with multi-color

2-1. Introduction

Heterotrimeric guanine nucleotide-binding proteins (heterotrimeric G proteins) are made up of three different subunits: alpha (Gα), beta (Gβ) and gamma (Gγ) subunits. They act as molecular switches inside cells, and their main function is signal transduction working together with G protein-coupled receptors (GPCR). When responds to a ligand-induced conformation change of GPCR, Gα of heterotrimeric G proteins dissociates from the Gβγ dimer and then activates effector proteins in particular signal transduction pathways, evoking downstream signaling cascades.

By the plasma membrane recruitment of constitutively active form of $G\alpha_q$ and $G\alpha_s$ using the chemically-inducible dimerization system: FKBP/FRB, it has been achieved in directly activating Gα bypass the GPCR, which induces downstream signaling cascades. However, the limitation of this approach is it hardly reaches spatiotemporal control because of the irreversibility and the diffusiveness of the chemical dimerization. In addition, optogenetic tools like optoXRs, which allow achieving high spatiotemporal precision, have also been developed for manipulation of Gα. The limitation of optoXRs is that they are usually incompatible with other fluorescent tools used as biomarkers or biosensors, because the excitation wavelength of these tools may potentially perturb the function of optoXRs which having broad absorption band. To address these problems, new optogenetic approaches to manipulate the heterotrimeric G proteins is required.

We anticipated that the translocation of Gα ($G\alpha_q$ and $G\alpha_s$) to the plasma membrane by a light dependent way rather than the chemical method should also be able to activate the effector of Gα. To achieve this purpose, we focused on approaches to active proteins using the photoswitches: Magnet system and PhyB/PIF6 system. We localized part A of the photoswitch to the plasma membrane by fusing it to a membrane localization sequence: CAAX motif[65], which is available to target proteins to the endomembrane of cell (Figure 2-1). In the other side, part B of the photoswitch is fused to the Gα expression in the cytoplasm. Upon the light illumination, the two parts of the photoswitch interact with each other, resulting in the translocation of Gα from cytoplasm to plasma membrane. The reaction is reversible because when switched to another light condition, the interaction between the photoswitch can be

blocked and the $G\alpha_q$/$G\alpha_s$ will release from the membrane to the cytoplasm again.

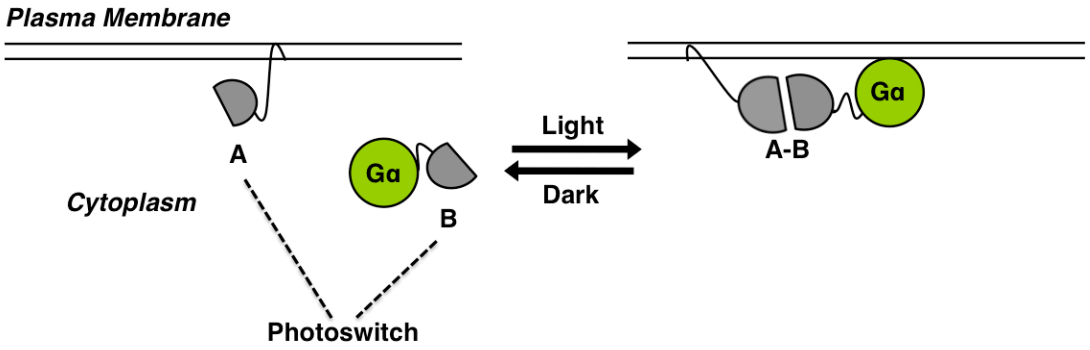

Figure 2-1. Translocation of heterotrimeric G proteins to plasma membrane.

There are different classes of Gα, the application of different photoswitches: blue light activatable Magent system and red light activatable PhyB/PIF6 system will allow us to achieve multi-color control of different Gα ($G\alpha_q$ and $G\alpha_s$) seperately. The attractive characteristic of light is that it has superior temporal and spatial resolution. The development of these optical approaches will achieve the regulation of second messengers with high spatiotemporal resolution.

2-2. Materials & Methods

2-2-1. DNA constructions

The humanized gene encoded variants of nMag/pMag were gifted from Dr. Kawano. The humanized genes encoded PhyB construct harboring tandem PAS (1-908) and 100-residue N-terminal phytochrome binding domain of PIF6 were synthesized by Eurofins Genemics (Tokyo, Japan). cDNAs encoding human $G\alpha_q$ and $G\alpha_s$ were gifted from Dr. Putyrski. All plasmid constructions appeared in this study were created by standard molecular biology techniques and separately subcloned into the mammalian expression vector pcDNA3.1. All cloning enzymes were obtained from Takara Biomedical (Tokyo, Japan) and used according to the manufacturer's instructions. The constructions were confirmed by sequencing the cloned fragments. Several mutants of protein (such as C9S and C10S mutants in $G\alpha_q$) were used in this research. The present mutagenesis was performed with an overlap extension technique and Multi Site-Directed Mutagenesis Kit (MBL, Nagoya, Aichi, Japan) according to the manufacturer's instructions.

2-2-2. Cell culture

COS-7 and HEK293 cells were cultured at 37°C under 5% CO_2 in Dulbecco's Modified Eagle Medium (DMEM; Invitrogen). HeLa cells were cultured under 5% CO_2 in Minimum Essential Medium Eagle (MEM; SIGMA). Both mediums were supplemented with 10% fetal bovine serum (GIBCO, Carlsbad, CA, USA), 100 unit/ml of penicillin and 100 μg/ml of streptomycin (GIBCO). These cells were for translocation assay, Ca^{2+} imaging and bioluminescence assay.

2-2-3. TIRF imaging

To conduct the plasma membrane-translocation assay of the activator construct using TIRF imaging[66], COS-7 cells were plated at 1.0 x 10^4 cells per dish on glass-bottomed dishes and cultured for 24 hours at 37 °C in 5% CO_2. The cells were transfected with

cDNAs encoding DsRedEx2-pMagFast1-$G\alpha_q$ and nMagHigh1-mKikGR-CAAX at a 1:1 ratio using X-tremeGENE 9 DNA transfection reagent (Roche Diagnostics GmbH, Mannheim, Germany) according to manufacturer's protocol. The total amount of DNA was 1 μg per dish. Twenty-four hours after transfection, the medium was replaced by the DMEM culture medium supplemented with 10% FBS. The cells were maintained for 24 hours at 28 °C. Before imaging, the culture medium was replaced with Hanks' Balanced Salt Solution (HBSS, Grand Island Biological Co., Grand Island, NY, USA) containing 10 mM HEPES. Imaging was performed at room temperature with a 100 × oil objective on the stage of an ECLIPSE Ti TIRF microscope (Nikon, Tokyo, Japan). Fluorescence images of DsRedEx2 were taken using an optically pumped semiconductor laser at 561 nm (Coherent, CA, USA). Blue light illumination was conducted using an optically pumped semiconductor laser (488 nm) at 1 mW for 50 ms.

2-2-4. Live cell imaging

The 35 mm glass-bottomed dishes (AGC TECNO GLASS Co., Shizuoka, Japan) were coated with poly-L-lysine (Sigma-Aldrich Co., Missouri, USA) at room temperature for 60 minutes, washed twice with 2 ml Milli-Q for use. As an example, HEK293 cells were plated at approximately 2.0×10^4 cells/dish and cultured for 24 hours at 37 °C with 5% CO_2. Cells were then transfected with cDNAs encoding nMagHigh1-mKikGR-CAAX, pMagFast1-$G\alpha_q$ and R-GECO1 or substitutions using X-tremeGENE 9 DNA transfection reagent. Twenty-four hours after transfection, the culture media were replaced with HBSS containing 10 mM HEPES. Live cell imaging was conducted at 37 °C with a heated stage adaptor (Tokai Hit Co., Fujinomiya, Shizuoka, Japan). Fluorescence images of mKikGR and R-GECO1 were taken using a solid-state laser at 515 nm (Coherent) and a laser diode at 559 nm (NTT electronics, Yokohama, Japan) respectively. Blue light illumination was completed with a Laser diode at 473 nm.

HeLa cells were plated in 35 mm glass bottom dish (MATSUNAMI, Tokyo, Japan) and seeded for 24 hours, achieving to approximately 70% confluence of the plate. cDNAs encoding PhyB-FusionRed-CAAX, PIF6-$G\alpha_q$ and GCaMP3 were transfected to cells at a ratio 3:1:1 using the Lipofectamine 3000 Transfection Kit (Invitrogen,

CA, USA) for 24 hours at 37°C. The total amount of DNA was 0.5 μg. The cells were further incubated for 12 hours at 28°C. PCB（Frontier Scientific, Logan, UT, USA）was added to the cells under dark condition to give a final concentration of 20 μM and incubated another 60 minutes. Then the culture media were washed and replaced with HBSS. Live cell imaging was conducted at 28°C with the heated stage adaptor. Fluorescence images of FusionRed and GCaMP3 were taken using a solid-state laser at 559 nm (NTT electronics, Yokohama, Japan) and a laser diode at 473 nm (Olympus, Tokyo, Japan) respectively. Red light illumination was completed with a laser diode at 635 nm (Olympus). LED array (735 nm ± 20 nm, 1.5 mW/cm^2) was used as the inactivation light. To monitor the plasma membrane recruitment of PIF6-Gα_q, mYFP (Q70K) was inserted between PIF6 and Gα_q. Translocation assay was performed under a same condition after PhyB-FusionRed-CAAX and PIF6-mYFP-Gα_q were transfected to HeLa cells at a 9:1 ratio.

FV1200 confocal laser scanning microscope (Olympus) and 60 × oil immersion objective were used in live cell fluorescence imaging and translocation assay.

2-2-5. Bioluminescence assay

HEK 293 cells were plated at approximately 1.0 × 10^5 cells/well in a 24-well plate (AGC TECNO GLASS Co., Shizuoka, Japan), and cultured for 24 hours at 37 °C with 5% CO_2. cDNAs encoding PhyB-FusionRed-CAAX, PIF6-Gα_s and the reporter pGL4.29 [luc2P/CRE/Hygro] were transfected to cells at a ratio 3.5:0.5:1 using the Lipofectamine 3000. The total amount of DNA was 0.5 μg/well. Then samples were covered with foil to ensure dark conditions and kept in 37°C incubator for 12 hours, an additional 12 hours incubation at 28°C was executed for enough protein accumulation and better membrane localization. PCB was dissolved in DMEM and added to the samples half an hour before illumination. We used LED light sources (CCS Inc., Kyoto, Japan) for red (660 ± 20 nm) and far-red (735 ± 20 nm) light illumination respectively. The culture medium was removed after a period of illumination. The cells were treated with 200 μl/well passive lysis buffer (Promega, Madison, WI, USA) for 15 minutes at room temperature. 500 μl HBSS culture medium containing 200 μM D-luciferin pottasium salt (Wako Pure Chemistry Industries, Ltd., Osaka, Japan) was prepared as a substrate. Bioluminescence

measurements were immediately performed after mixing the D-luciferin solution with the lysed cells using a Glomax 20/20 Luminometer at room temperature (Promega).

2-3. Results

2-3-1. Blue light-induced membrane recruitment of $G\alpha_q$.

Magnet system consisting of nMagHigh1 and pMagFast1 is a recently developed dimerization system, which is based on a photoreceptor Vivid derived from Neurospora crassa. Heterodimerization occurs between nMagHigh1 and pMagFast1 upon blue light illumination, while moved to darkness, the interaction dissociates quickly. The Magnet system shows high interaction affinity and fast switch-off kinetic, absorbs a narrow spectrum of blue light and its heterodimerization can be induced with weak light power. These facilitative properties of the Magnet system show the feasibility to gain precise spatiotemporal control of Gα. In utilization of the photoswitchable Magnet system, we designed a strategy (Figure 2-2) that blue light induces $G\alpha_q$ to move from the cytoplasm toward the plasma membrane, where $G\alpha_q$ activates the effector phospholipase C-beta (PLCβ) and triggers the cytosolic Ca^{2+} release. In this translocation-based approach, pMagFast1 linked with $G\alpha_q$ at the C-termini is localized in the cytoplasm, while nMagHigh1 tagged with mKikGR is anchored to the plasma membrane using a membrane localization sequence: CAAX motif. The fluorescent protein mKikGR[67] can be used to monitor the expression level of the probe and mark the cells of interest. After blue light stimulation, heterodimerization occurs between nMagHigh1 and pMagFast1, and thereby induces the translocation of pMagFast1-linked $G\alpha_q$ from the cytoplasm to the plasma membrane. The translocation of $G\alpha_q$ to the plasma membrane activates the downstream effector PLCβ, which produces inositol 1,4,5-triphosphate (IP3) and diacylglycerol (DAG). Subsequently, IP3 binds to IP3 receptor (IP3R) on endoplasmic reticulum (ER) and leads to the release of Ca^{2+} from the intracellular store sites to the cytosol.

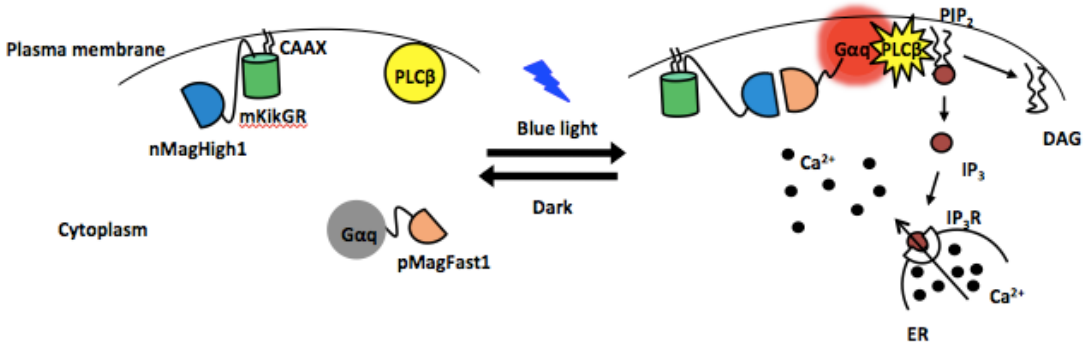

Figure 2-2. Light-inducible dimerization of the Magnet system allows $G\alpha_q$ to translocate to the plasma membrane and trigger cytosolic Ca^{2+} release through the phospholipase C-beta (PLCβ)-inositol triphosphate receptor (IP_3R) pathway.

To confirm the blue light-dependent interaction between nMagHigh1 and pMagFast1, we performed the cell-based translocation assay using a total internal reflection fluorescence (TIRF) microscope. nMagHigh1-mKikGR-CAAX and DsRedEx2-pMagFast1-$G\alpha_q$ were coexpressed in COS-7 cells. mKikGR and DsRedEx2 were fluorescence proteins visualizing the expression of the two constructions. nMagHigh1 was targeted to the plasma membrane using the membrane localization sequence CAAX while pMagFast1 was targeted to the cytoplasm at first. We traced the fluorescence intensity of DsRedEx2[68] in the plasma membrane and observed a remarkable increase of TIRF signal directly after 488 nm (blue) laser illumination (Figure 2-3). In order to verify the light dependency of the fluorescence change, we introduced C71S[20] mutation to nMagHigh1 and pMagFast1, which impairs the photoswitching dimerization of these two proteins. As expected, the C71S substitutions generated scarcely TIRF signal change upon 488 nm light illumination. These results demonstrate that the dimerization of nMagHigh1 and pMagFast1 is switched on upon blue light illumination, and this blue light-dependent dimerization is able to induce the recruitment of cytosolic DsRedEx2-pMagFast1-$G\alpha_q$ to the nMagHigh1-decorated plasma membrane.

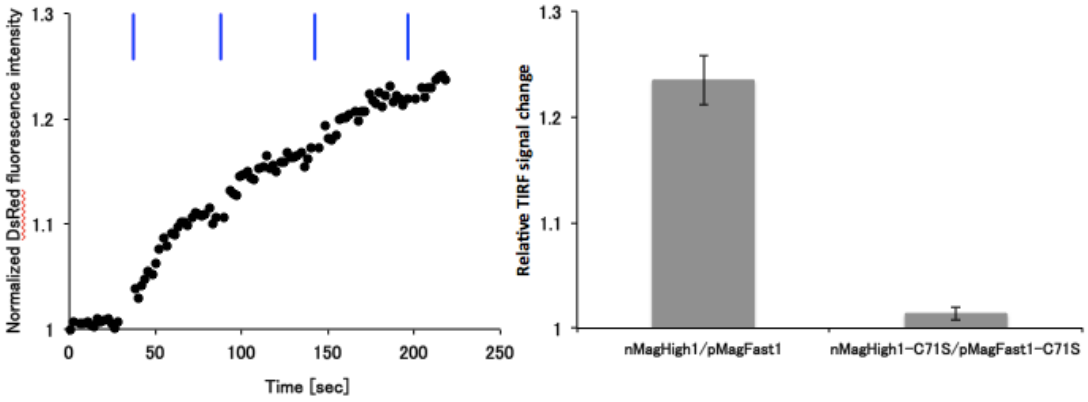

Figure 2-3. TIRF translocation assay. (Left) nMagHigh1-mKikGR-CAAX and DsRedEx2- pMagFast1-$G\alpha_q$ were co-expressed in COS-7 cells. The fluorescence intensity was significantly increased after blue light stimulation at 488 nm (blue bar). (Right) The Magnet system-based probe (nMagHigh1/pMagFast1) showed a remarkable TIRF signal change upon the blue light illumination while negative mutants with C71S substitutions (nMagHigh1-C71S/pMagFast1-C71S) showed no significant TIRF signal change after the blue light stimulation.

2-3-2. Blue light-induced Ca^{2+} release.

nMagHigh1-mKikGR-CAAX and pMagFast1-$G\alpha_q$ were transfected to the human embryonic kidney 293 (HEK 293) cells. As confirmed by the fluorescence of mKikGR, nMagHigh1 domain was anchored to the plasma membrane (Figure 2-4). To quantify the Ca^{2+} level induced by activated $G\alpha_q$, we transfected a Ca^{2+} indicator R-GECO1[69], which was excited at 559 nm spectrally distinct from the absorption spectrum of the Magnet system.

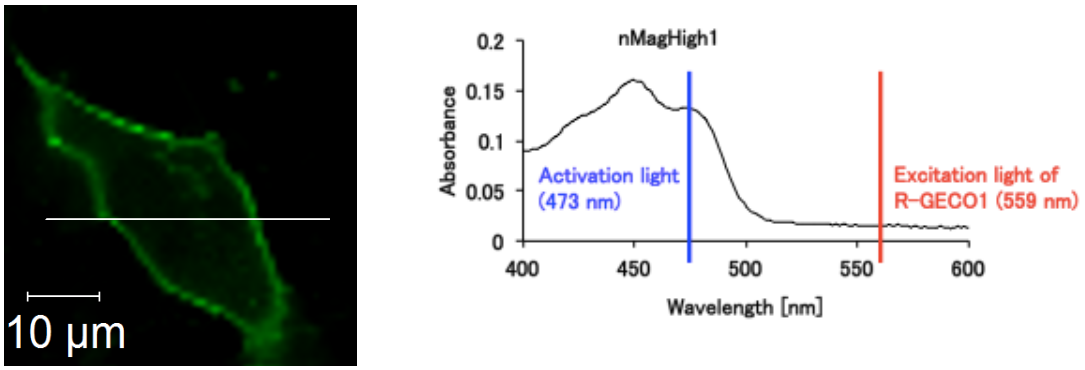

Figure 2-4. (Left) Membrane localization of nMagHigh1-mKikGR-CAAX; (Right) Absorption spectrum of purified nMagHigh1 protein. Blue line stands for the activation light used for the dimerization of Magnet system. Red line stands for the excitation light used for the fluorescence imaging of R-GECO1.

Ca^{2+} responses were transiently evoked in the cells immediately after nMagHigh1 and pMagFast1 were activated upon blue light illumination at 473 nm (Figure 2-5). This result demonstrates that blue light-dependent membrane recruitment of pMagFast1-$G\alpha_q$ induces the Ca^{2+} release in the cells. In contrary, cells in the absence of the light stimulation failed to detect any Ca^{2+} response, implying the excitation light (559 nm) for R-GECO1 did not perturb the interaction of the Magnet system as expected from its absorption spectrum.

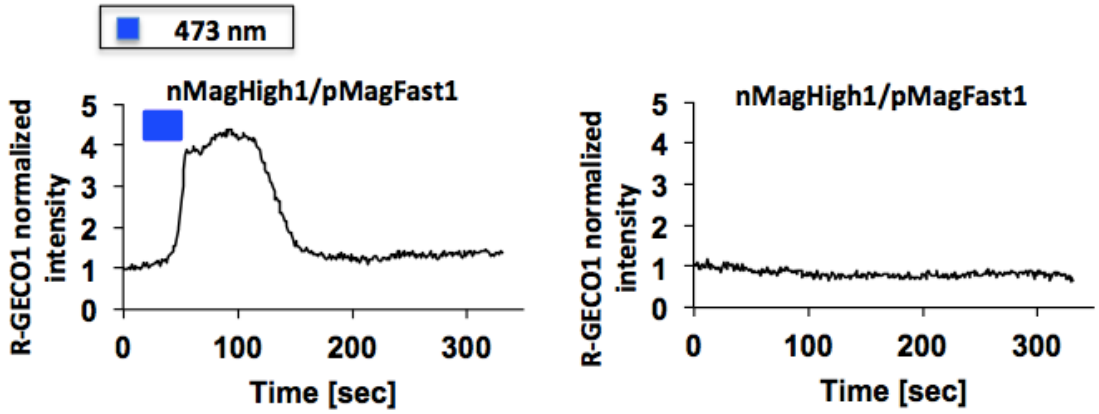

Figure 2-5. Ca^{2+} responses with (left) or without (right) blue light stimulation in the Magnet system based probe.

There was not any blue light-dependent response observed in the negative control that cells only expressing R-GECO1 (Figure 2-6). We also did not detect any Ca^{2+} signal under the blue light illumination when the C71S substitutions were employed to this approach, which well explained the light dependence of this approach.

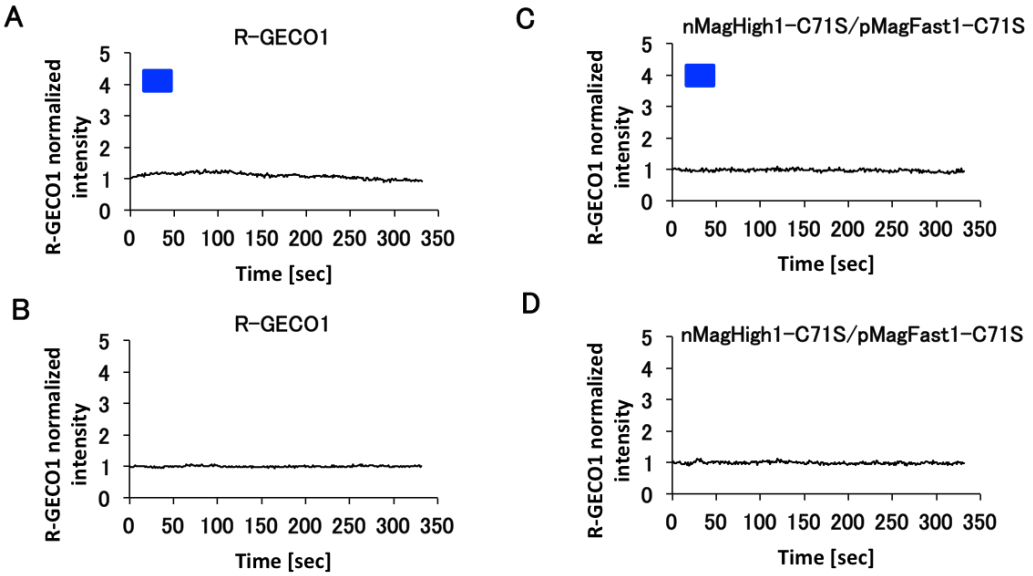

Figure 2-6. Negative controls of blue light-induced $G\alpha_q$ system. When only the Ca^{2+} indicator R-GECO1 was transfected to cells, no signal was evoked with (A) or without (B) blue light stimulation. By introducing the C71S inactive mutations, Ca^{2+} signal was not evoked with (C) or without (D) blue light stimulation. Blue bars indicate blue light illumination at 473 nm.

Next we compared the Magnet-based approach with the corresponding Ca^{2+} modulating tool of optoXRs called opto-α1AR. Live cell imaging was conducted after

R-GECO1 and opto-α1AR were co-expressed in HEK 293 cells. Similarly, 473 nm laser light was illuminated to the specially designated regions as the stimulation source of opto-α1AR. We recorded the time-lapse cytosolic fluorescence intensity of R-GECO1. As a result, the response of R-GECO1 was observed with or without 473 nm light illumination in opto-α1AR (Figure 2-7). This experiment yields that opto-α1AR is activated by the excitation light of R-GECO1 because rhodopsin covers a broad absorption band, thereby resulting in undesired Ca^{2+} oscillations.

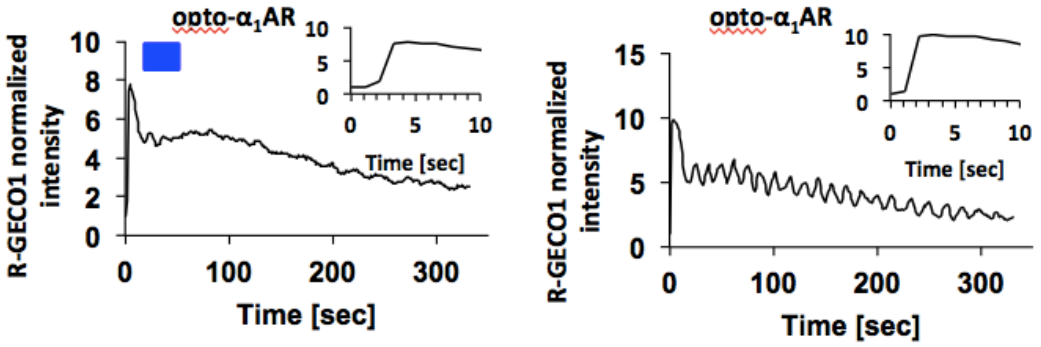

Figure 2-7. Ca^{2+} responses with (left) or without (right) blue light stimulation in opto-α1AR.

By the direct comparison between the Magnet-based approach and opto-α1AR, we conclude that our strategy affords advantage in selectable usage of photoswitchable dimerization systems having narrow absorption spectrums, such as the Magnet system in this case, which indeed leads to the incorporation with R-GECO1 rending it more implementable for Ca^{2+} imaging.

To evaluate the repeatability of this approach, 473 nm laser light was illuminated to the same cell scheduling 5-10 minutes interval for a total of 100 minutes and every time Ca^{2+} signal was captured by R-GECO1 (Figure 2-8). The blue light-dependent oscillations show that the regulation of the membrane recruitment of $G\alpha_q$ and the subsequent release of Ca^{2+} can be repeatedly manipulated with blue light without losing the efficiency. We further certify that the manipulation of intracellular Ca^{2+} level is spatially photo-regulated. Upon blue light illumination, the fluorescence intensity of R-GECO1 in the specified cell was increased, indicating a higher intracellular Ca^{2+} level upon blue light stimulation. While the fluorescence brightness of R-GECO1 generally remained unchanged in the other cells without exposure to blue light, showing that the present system is suitable to space-resolved activation of

Ca^{2+} release. Additionally, the amplitude of calcium spikes after blue light illumination showed comparable to that elicited by ligand-induced activation of endogenous histamine receptor (Figure 2-9).

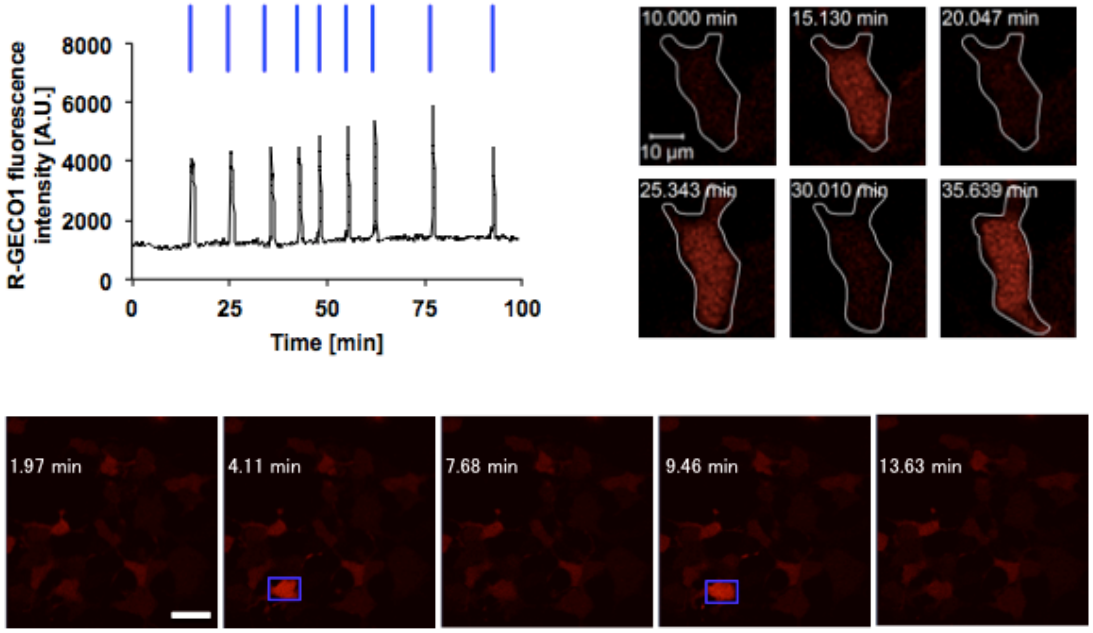

Figure 2-8. Ca^{2+} imaging using the Magnet-based approach with pulsed blue light illumination. Time-lapse fluorescence imaging showed that repeatable response of R-GECO1 was evoked upon activation light at 473 nm. Blue bars indicate 473 nm laser illumination(upper panel). Only the specified region (blue rectangle) illuminated with blue light at 488 nm showed Ca^{2+} release. Scale bar 50 μm（lower panel）.

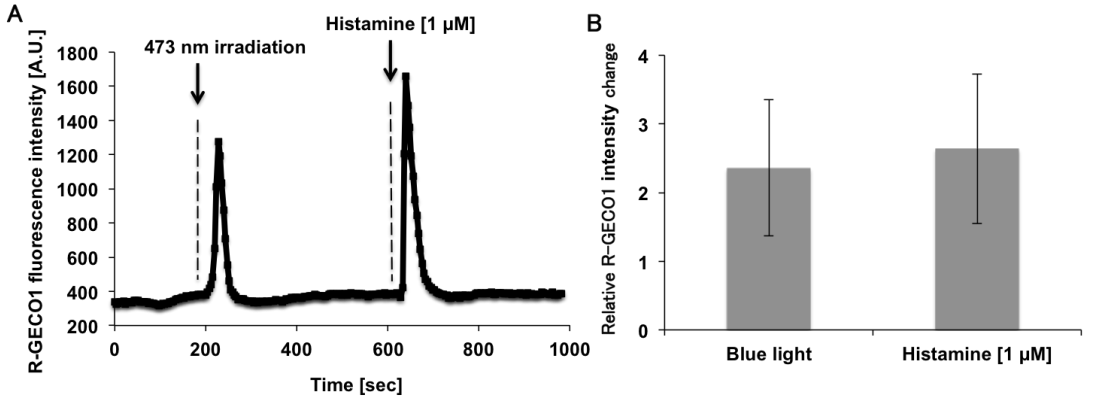

Figure 2-9. Comparison of blue light-induced Ca^{2+} response with histamine-induced Ca^{2+} response. (A) Measurement of fluorescence intensity of R-GECO1 upon different stimulations with blue light (B) Averaged amplitude of R-GECO1 fluorescence intensity by blue light illumination (n=10) or histamine stimulation (n=12).

2-3-3. Red light-induced Ca^{2+} release.

Another advantage of the present strategy over the optoXRs is that $G\alpha_q$ can also be manipulated by different wavelength of light via replacing the Magnet system to other types of dimerization system. Here I present another optogenetic approach to manipulate $G\alpha_q$ based on the red light-inducible PhyB/PIF6 system.

The PhyB/PIF6 system is sensitive to red light for binding, and shows low binding affinity in darkness or under far-red illumination. FusionRed-tagged PhyB is anchored to the plasma membrane by tethering to CAAX while PIF6 linked with $G\alpha_q$ is targeted to the cytoplasm. After red light stimulation, the plasma membrane-anchored PhyB binds to the $G\alpha_q$-linked PIF6, and thus leads to the translocation of PIF6-$G\alpha_q$ from the cytoplasm to the plasma membrane, where the $G\alpha_q$ activates PLCβ and subsequently evokes the Ca^{2+} releasing to the cytosol. When under far-red condition, PIF6-Gαq dissociates from the plasma membrane to the cytoplasm, blocking the Ca^{2+} release (Figure 2-10).

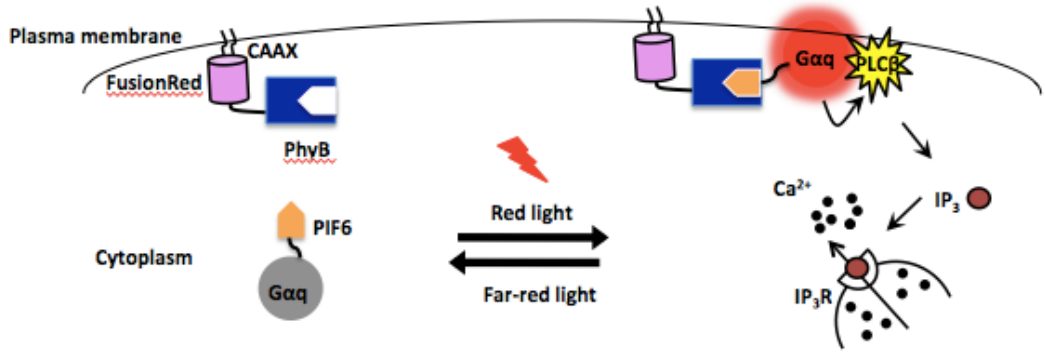

Figure 2-10. Red light-inducible dimerization of the PhyB/PIF6 system allows the plasma membrane recruitment of $G\alpha_q$ and triggers cytosolic Ca^{2+} release.

For confocal imaging of the plasma membrane translocation of the PhyB/PIF6-based photoswitch, PhyB-FusionRed-CAAX and PIF6-mYFP-$G\alpha_q$ were transfected to HeLa cells. Upon stimulation with red light (635 nm), the calculated fluorescence intensity of mYFP[70] in the cytosol was decreased, while it was increased in the plasma membrane (Figure 2-11), suggesting the red light-induced recruitment of PIF6-mYFP-$G\alpha_q$ to the plasma membrane. Previous researches show that the dissociation of PhyB/PIF6 interaction not only occurs under far-red illumination but

also takes place in darkness with very likely different kinetics and it is clear that far-red light-induced PhyB/PIF6 dissociation is much faster than the dark reversion rate.

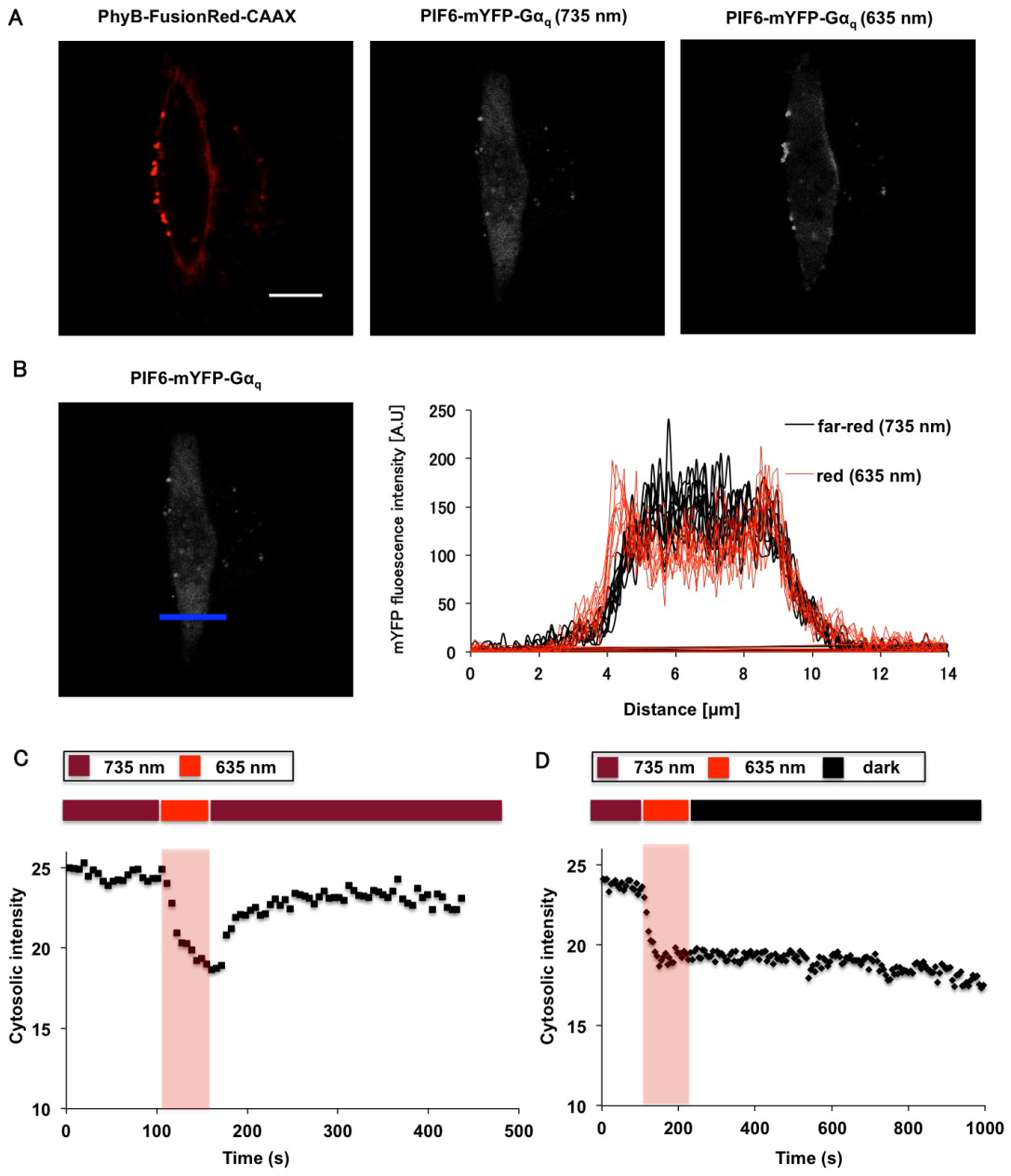

Figure 2-11. Translocation of the PhyB/PIF6-based photoswitching system. (A) Expression of PhyB-FusionRed-CAAX and PIF6-mYFP-Gα_q. Scale bar, 10 µM. The fluorescence intensity of mYFP increased in the plasma membrane upon stimulation with red light at 635 nm, demonstrating the translocation of PIF6-mYFP-Gα_q to the plasma membrane. (B) Line profiles (right panel) represent fluorescence intensity of mYFP measured along the blue line of the PIF6-mYFP-Gα_q image (left panel). (C) Cytosolic fluorescence of mYFP was immediately increased after far-red illumination suggesting

that far-red induced PhyB/PIF6 dissociation quickly. (D) There was no cytosolic fluorescence increase in the short period time under dark condition.

I employed GCaMP3[71] as the Ca^{2+} indicator and excited it at 473 nm to avoid the interference to the PhyB/PIF6 interaction. PhyB-FusionRed-CAAX, PIF6-Gα_q and GCaMP3 were transfected to HeLa cells. It is evident that GCaMP3 was homogeneously dispersed in the cytoplasm and the PhyB domain was anchored to the plasma membrane (Figure 2-12). During the Ca^{2+} imaging with GCaMP3 at 473 nm, far-red (735 nm) and red (635 nm) light was alternatively used to control the dissociation and association of PhyB/PIF6. In accordance with the result of the Magnet-based approach, Ca^{2+} signal could be repeatedly evoked in the cells upon red light illumination at 635 nm. Negative controls in the absence of PhyB-FusionRed -CAAX or PIF6-Gα_q did not show any red light-dependent Ca^{2+} response. These results demonstrate that our strategy allows selective utilization of different photoswitchable dimerization systems to manipulate the membrane recruitment of Gα_q and light-induced Ca^{2+} release.

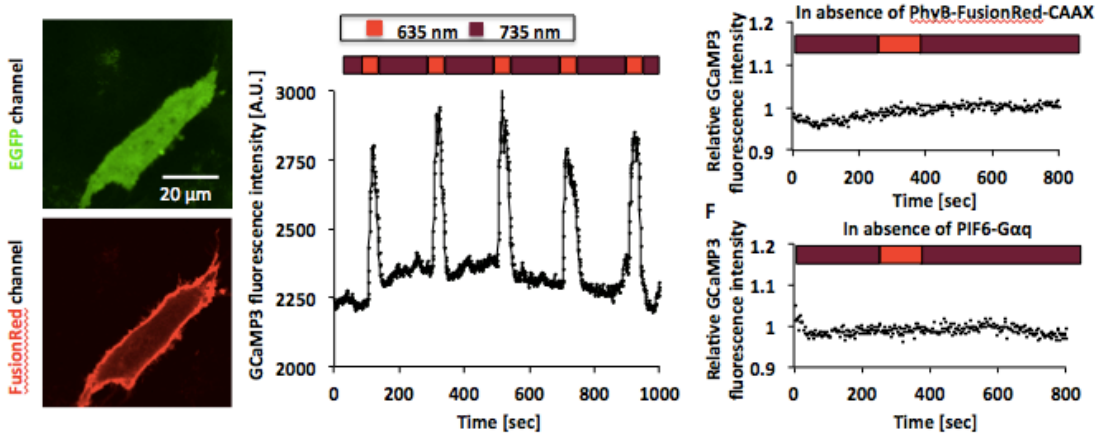

Figure 2-12. (Left) Homogeneous cellular diffusion of GCAMP3 in HeLa cell (upper panel) and the plasma membrane localization of PhyB-FusionRed-CAAX (lower panel). (Middle) Ca^{2+} imaging of the PhyB/PIF6-based approach with pulsed red light illumination. Time-lapse fluorescence imaging showed that repeatable response of GCAMP3 was evoked upon activation light at 635 nm (red bars), 735 nm far-red (deep red bars) illumination was used as the inactivation light. (Right) Negative control in the absence of PhyB-FusionRed-CAAX did not show red light-dependent response.

2-3-4. Red light-induced cAMP increase.

Varieties of Gα appropriate different downstream effectors in the plasma membrane. As previously mentioned, the manipulation of the $G\alpha_q$ leads to the release of cytosolic Ca^{2+}. I sought to extend the strategy by the replacement of PIF6-linked $G\alpha_q$ to $G\alpha_s$. $G\alpha_s$ activates the downstream adenylyl cyclase (AC) after its localization at the plasma membrane and catalyzes the conversion of adenosine triphosphate (ATP) to 3′, 5′-cyclic AMP (cAMP) and pyrophosphate[72, 73].

I employed cAMP response element (CRE) driven secretory luciferase construct PCRE-luc[74] as a reporter to test whether light-actuated recruitment of $G\alpha_s$ to the plasma membrane will increase the cAMP level in living cells. cAMP regulates the transcription of the downstream luciferase gene via a conserved gene promoter element CRE (Figure 2-13). Theoretically, a higher intracellular cAMP level leads to a greater expression of luciferase, which can be sensitively measured by the luminescence intensity.

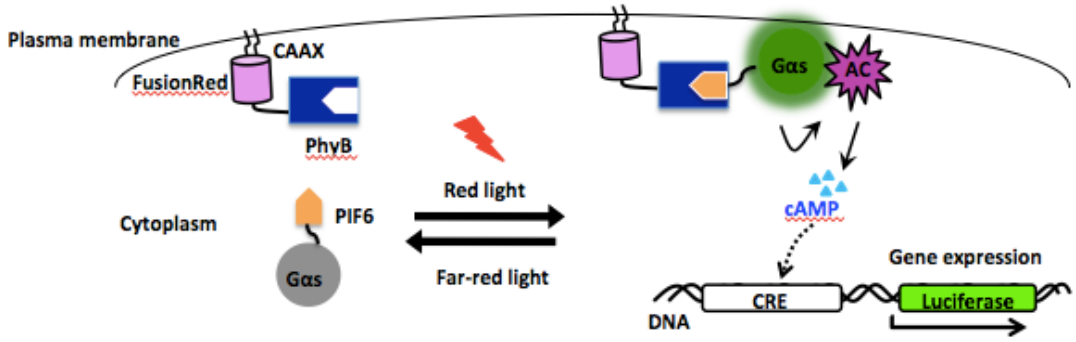

Figure 2-13. Red light-inducible dimerization of the PhyB/PIF6 system allows $G\alpha_s$ to translocate to the plasma membrane and trigger cAMP release owning to the activation of adenylyl cyclase (AC).

PhyB-FusionRed-CAAX, PIF6-$G\alpha_s$ and PCRE-luc were transfected to HEK293 cells, and the cells were kept in a dark incubator for protein expression before exposure to light. I measured the cAMP level by tracing the luminescence intensity of the CRE-driven gene expression products. The luminescence intensity of samples under the far-red light (735 nm) condition remains constant (Figure 2-14), which reveals far-red illumination kept the intracellular cAMP in a roughly invariant level. Conversely, the luminescence intensity of the samples under the red light (660 nm)

condition significantly increased after the beginning of the illumination and reached a maximum value in about 15 hours. This result indicates that red light-triggered recruitment of $G\alpha_s$ generates a higher intracellular cAMP level that is sufficient to facilitate the gene expression. The incorporation of cofactor phytochromobilin (PΦB) or phycocyanobilin (PCB) is required for the light sensitivity of PhyB[75]. As expected, the luminescence intensity of samples in absence of cofactor PCB did not increase even under red light illumination. Further analysis about the correlation between PCB concentration and the PhyB/PIF6-induced cAMP level suggested that 50 μM is preferable under the conditions we used.

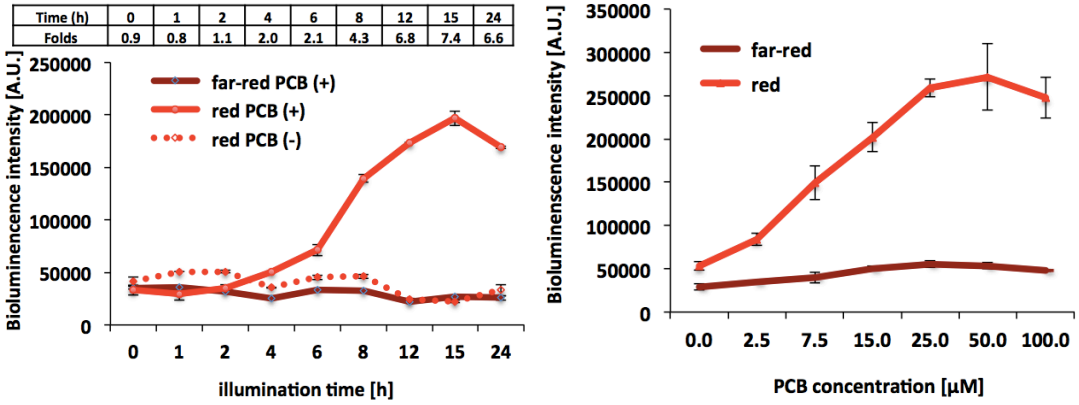

Figure 2-14. (Left) Time-lapse luminescence intensity of samples under red illumination at 660 nm (red) or far-red illumination at 735 nm (far-red), with (PCB (+)) or without (PCB (-)) addition of PCB. The increment of luminescence intensity was only observed in the samples under red illumination in the presence of PCB. The upper table means the normalized intensity ratio changes between red PCB (+) and far-red PCB (+). (Right) Relationship between PCB concentration and the luminescence intensity.

Moreover, I measured the red power dependency against the luminescence intensity. The result indicates that the cAMP level is precisely fine-tuned by varying the red light power between 0.01 mW/cm^2 and 1 mW/cm^2 (Figure 2-15). Finally optimization of several parameters including PCB concentration, illumination time and light power allowed a 14-fold bioluminescence intensity difference between the samples under red (660 nm) and far-red (735 nm) light conditions. Besides, the samples kept in darkness showed a similar result to those illuminated by far-red light, which is consistent with the fact that both dark and far-red conditions make PhyB binding with its partner PIF6 in a low affinity. As a negative control, cells without expressing

PhyB-FusionRed-CAAX showed very faint luminescence and appeared no appreciable difference between red and far-red conditions.

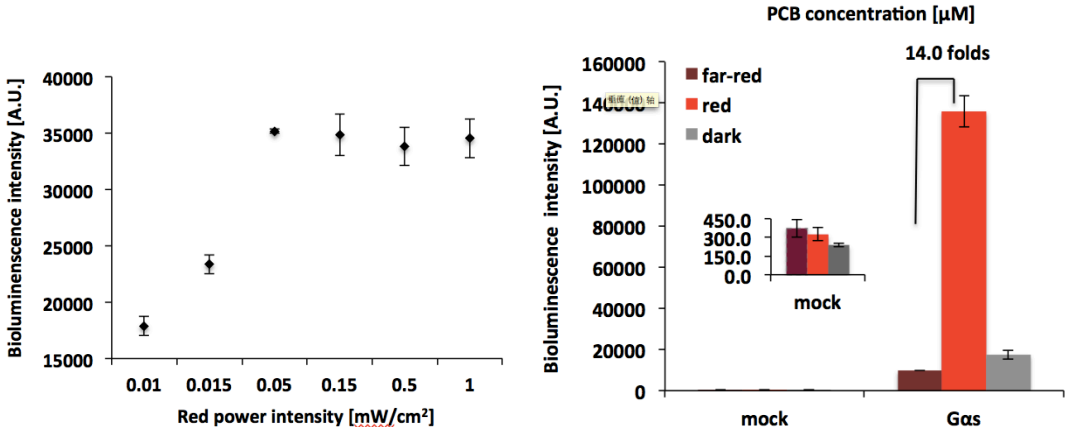

Figure 2-15. (Left) Power dependency of the luminescence intensity under illumination at 660 nm. (Right) Result of the bioluminescence assay after optimization of several parameters including PCB concentration (50 µM), illumination time (14 hours) and light power (red: 0.15 mW/cm^2; far-red: 1.5 mW/cm^2). The inset is a partially enlarged view of Mock, which means a negative control in the absence of PhyB-FusionRed-CAAX.

Additionally, I showed that the red light-induced cAMP increase with the PhyB/PIF6-based Gα_s system is more significant than cAMP increase stimulated by endogenous GPCR ligands and the effect is approximately equivalent to the result when 5 µM foskolin was tested (Figure 2-16). Based on all the calculated results, it is proved that optical manipulation of Gα using our strategy is not merely applicable to Gα_q but also suited for Gα_s.

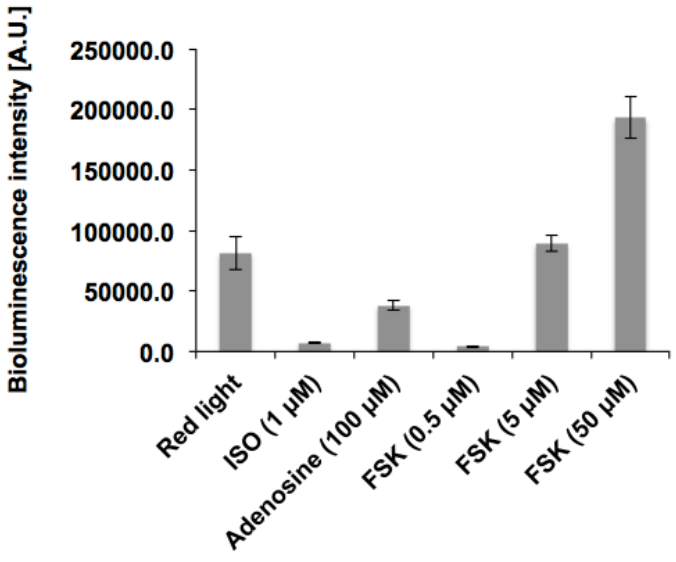

Figure 2-16. Comparison of different stumili-responsive cAMP level: red light, native GPCR ligands

and forskolin. HEK 293 cells transfected with PhyB-FusionRed-CAAX, PIF6-Gα_s and reporter gene (P_{CRE}-luc), and the bioluminescence intensity was measured 12 hours after red light illumination (660 nm, 0.15 mW/cm^2). While other cells were transfected with reporter only but cheated with 1 μM isoprenaline (ISO), 100 μM adenosine and different concentration (0.5, 5, 50 μM) of forskolin (FSK). The error bars indicate standard deviation from three individual samples.

2-4. Discussion & Conclusion

In this study, we developed and certified a strategy that Gα achieves activation via light-controlled translocation of Gα from the cytoplasm to the plasma membrane using photoswitchable dimerization systems. In contrast to optoXRs, this strategy affords unique advantage in selectable usage of photoswitchable dimerization systems having narrow absorption spectrums, thereby allowing the feasibility of combinational application with other fluorescent tools. Additionally, this strategy is generally applicable to different classes of Gα. To be more specific, we demonstrated individual approaches to manipulate $G\alpha_q$ and $G\alpha_s$ based on the Magnet system and the PhyB/PIF6 system, and the light-dependent regulation of two second messengers: Ca^{2+} and cAMP.

Our strategy provides multiple selections of dimerization system to manipulate Gα in order to meet the demands of different applications. We demonstrate that the wavelength used in light-triggered recruitment of the $G\alpha_q$ can be easily shifted from blue (473 nm) to red (635 nm) by replacing the dimerization systems. Both two approaches achieve temporal and repeatable regulation of cytosolic Ca^{2+} release upon photoirradiation. These two different dimerization systems have their own features. The Magnet system has high interaction affinity and an exogenous addition of cofactor is not required. The PhyB/PIF6 system has fast switch-off kinetic and it should be superior when applied to in vivo studies because of the better tissue penetration of red light. Regardless of which approach is used, it should be emphasize that the most remarkable characteristic for manipulation of $G\alpha_q$ with the Magnet system and the PhyB/PIF6 system is the competitive advantage over the opto-α_1AR. Opto-α_1AR getting broad absorption band suffers from the perturbation by the excitation light for Ca^{2+} indicators. The use of the Magnet system or the PhyB/PIF6 system that has narrow absorption band overcomes this fundamental difficulty. These photoswitching systems are supposed to free up vacant spectrum that provide more selection of fluorescent proteins for labeling. This distinct spectral property also can be harnessed to combine with other optogenetic tools such as channelrhodpsin-2 [4, 76].

The successful manipulation of both $G\alpha_q$ and $G\alpha_s$ demonstrates that our strategy is feasible to optically manipulate different classes of Gα. Light-dependent control of

Ca^{2+} and cAMP has been achieved through the corresponding activation of $G\alpha_q$ and $G\alpha_s$. Optical regulation of these second messenger molecules provides extensive applications to mediate biological process. Moreover, optical recruitment of other classes of Gα as well as $G\alpha_q$ and $G\alpha_s$ to the plasma membrane may also be applicable by indiscriminately apply this strategy, and the property of 'auto-activation' upon the plasma membrane recruitment can be shared to all other classes of Gα, because they are generally believed to carry out signal functions at the plasma membrane. Therefore, diversified downstream pathways presumably can be regulated so as to mediate various patterns of signaling events in mammalian cells.

In summary, we provide a strategy to construct highly versatile approaches to optically manipulate the Gα. Various types of Gα can be recruited to the plasma membrane using different dimerization systems so as to reach the activation. As the functional application of this strategy, it enables optical switchable regulation of different second messengers in mammalian cells.

Chapter 3: Development of an affibody-based engineered system to switch cellular processes

（内容非公表）

Chapter 4: General conclusion

（内容非公表）

Acknowledgements

The present thesis study has been carried out under the supervision of Professor Moritoshi Sato. It is wonderful experience for me to study in his laboratory during the past several years. I would like to express my great appreciation for his considerable support for my graduate study. I am most grateful to him for his guidance, encouragement, and help throughout this study. The productive discussion with him was indispensable in the present study.

I sincerely appreciate Mr. Onodera and Mr. Aono for their great assistance. They contributed indispensable efforts to the study in chapter 2.

I also greatly appreciate Dr. Shimizu for his enthusiastic teaching, scientific supporting and valuable discussion throughout the study of ribosome display.

My special thanks are due to all the members in the Sato Moritoshi's laboratory for their stimulating discussion. Especially Dr. Nakajima, Dr. Ueda, Dr. Kawano, Dr. Suzuki, Dr. Otabe. They provided me very helpful advices and suggestions for the improvement of my study.

I also appreciate and make a special statement that China Scholarship Council (CSC) granted me the financial support during the year 2014-2018.

Finally, I would like to sincerely thank my family from the bottom of my heart for providing me with an opportunity to go to the graduate school, and for supporting my school life.

References

1. Michael H. Optogenetics: the age of light. *Nat. Methods* 11, 1012-1014 (2014).
2. Oesterhelt D. and Stoeckenius W. Rhodopsin-like protein from the purple membrane of halobacterium halobium. *Nat. New Biol.* 233, 149-152 (1971).
3. Matsuno-Yagi A. and Mukohata Y. Two possible roles of bacteriiorhodopsin; a comparative study of strains of Halobacterium halobium differing in pigmentation. *Biochem. Biophys. Res. Commun.* 78, 237-243 (1977).
4. Nagel G. et al. Channelrhodopsin-2, a directly light-gated cation-selective membrane channel. *Proc. Natl. Acad. Sci. USA* 100, 13940-13945 (2003).
5. Boyden E.S. and Deisseroth K. Millisecond-timescale, genetically targeted optical control of neural activity. *Nat. Neurosci.* 8, 1263-1268 (2005).
6. Petreanu L. et al. Channelrhodopsin-2-assisted circuit mapping of long-range callosal projections. *Nat. Neurosci.* 10, 663-668 (2007).
7. Tsai H.C. et al. Phasic firing in dopaminergic neurons is sufficient for behavioral conditioning. *Science* 324, 1080-1084 (2009).
8. Levskaya A. et al. Spatiotemporal control of cell signalling using a light-switchable protein interaction. *Nature* 461, 997-1001 (2009).
9. Karl D. Optogenetics. *Nat. Methods* 8, 26-29 (2011)
10. Gradinaru V. and Deisseroth K. Optical deconstruction of parkinsonian neural circuitry. *Science* 324, 354-359 (2009).
11. Airan R.D. et al. Temporally precise in vivo control of intracellular signaling. *Nature* 458, 1025-1029 (2009).
12. Wu Y.I. et al. A genetically encoded photoactivatable Rac controls the motility of living cells *Nature* 461, 104-108 (2009).
13. Toettcher J.E. et al. The promise of optogenetics in cell biology: interrogating molecular circuits in space and time. *Nat. Methods* 8, 35-38 (2011).
14. Jinek M. et al. A programmable dual-RNA-guided DNA endonuclease in adaptive bacterial immunity. *Science* 337 (6096), 816-821(2012).
15. Nagy A. Cre recombinase: the universal reagent for genome tailoring. *Genesis* 26 (2), 99-109 (2000).

16. Nihongaki Y. et al. Photoactivatable CRISPR-Cas9 for optogenetic genome editing. *Nat. Biotechnol*. 33(7), 755-760 (2015).
17. Kawano F. et al. A photoactivatable Cre-loxP recombination system for optogenetic genome *Nat. Chem. Biol*. 12(12), 1059-1064 (2016).
18. Gales C. et al. Real-time monitoring of receptor and G-protein interactions in living cells. *Nat. Methods* 2, 177-184 (2005).
19. Wettschureck N. and Offermanns S. Mammalian G proteins and their cell type specific functions. *Physiol. Rev*. 85, 1159-1204 (2005).
20. Banaszynski L. A., Liu C. W. and Wandless T. J. Characterization of the FKBP Rapamycin·FRB Ternary Complex. *J. Am. Chem. Soc*. 127, 4715-4721 (2005).
21. Putyrski M. and Schultz C. Switching heterotrimeric G protein subunits with a chemical dimerizer. *Chem. Biol*. 18, 1126-1133 (2011).
22. Putyrski M. and Schultz C. Protein translocation as a tool: The current rapamycin story. *FEBS Lett*. 586, 2097-2105 (2012).
23. Lin Y. et al. Rapidly reversible manipulation of molecular activity with dual chemical dimerizers. *Angew. Chem. Int. Edn Engl*. 52, 6450-6454 (2013).
24. Nakai J., Ohkura M. and Imoto K. High signal-to-noise Ca^{2+} probe composed of a single green fluorescent protein. *Nat. Biotechnol*. 19(2), 137-41 (2001).
25. Jasper A. et al. Optimization of a GCaMP calcium indicator for neural activity imaging. *J. Neurosci*. 32(40), 13819-13840 (2012).
26. Ohkura M. et al. Genetically encoded green fluorescent Ca^{2+} indicators with improved detectability for neuronal Ca^{2+} signals. *PLoS One*. 7(12), e51286. (2012).
27. Kennis J.T. et al The LOV2 Domain of Phototropin: A Reversible Photochromic Switch. *J. Am. Chem. Soc*. 126(14), 4512-4513(2004).
28. Guntas G. et al. Engineering an improved light-induced dimer (iLID) for controlling the localization and activity of signaling proteins. *Proc. Natl. Acad. Sci. USA* 112(1), 112-117 (2015).
29. Liu H. et al. Photoexcited CRY2 Interacts with CIB1 to Regulate Transcription and Floral Initiation in *Arabidopsis*. *Science* 322(5907), 1535-1539 (2008).
30. Kawano F. et al. Engineered pairs of distinct photo-switches for optogenetic control of cellular proteins. *Nat. Commun*. 6, 6256 (2015).
31. Michael S. et al. An optomechanical transducer in the blue light receptor

phototropin from *Avena sativa*. *Proc*. *Natl*. *Acad*. *Sci*. *USA* 98 (22), 12357-12361(2001).

32. Dougan D.A., Weber-Ban E. and Bukau B. Targeted delivery of an ssrA-tagged substrate by the adaptor protein SspB to its cognate AAA+ protein ClpX. *Mol*. *Cell* 12, 373-380 (2003).
33. Zoltowski B. D. et al. Conformational switching in the fungal light sensor Vivid. *Science* 316, 1054-1057 (2007).
34. Levskaya A. et al. Spatiotemporal control of cell signalling using a light-switchable protein interaction. *Nature* 461, 997-1001 (2009)
35. Konrad M. et al. A red/far-red light-responsive Bi-stable toggle switch to control gene expression in mammalian cells. *Nucleic Acids Res*. 41, e77 (2013).
36. Takala H. et al. Light-induced changes in the dimerization interface of bacteriophytochromes. *J*. *Biol*. *Chem*. 290, 16383-16392 (2015).
37. Beyer H.M. et al. Red light-regulated reversible nuclear localization of proteins in mammalian cells and zebrafish. *ACS Synth*. *Biol*. 4, 951-958 (2015).
38. Li F.W. et al. Phytochrome diversity in green plants and the origin of canonical plant phytochromes. *Nat*. *Commun*. 6, 7852 (2015).
39. Kojadinovic M. et al. Dual role for a bacteriophytochrome in the bioenergetic control of *Rhodopseudomonas palustris*: enhancement of photosystem synthesis and limitation of respiration. *Biochim*. *Biophys*. *Acta* 1777, 163-172 (2008).
40. Kaberniuk A.A., Shemetov A.A. and Verkhusha V.V. A Bacterial phytochrome-based optogenetic system controllable with near-infrared light. *Nat*. *Methods* 13(7), 591-597 (2016).
41. Taras A.R. et al. Near-infrared optogenetic pair for protein regulation and spectral multiplexing. *Nat*. *Chem*. *Biol*. 13(6), 633-639 (2017).
42. Smith G.P. Filamentous fusion phage: novel expression vectors that display cloned antigens on the virion surface. *Science*. 228 (4705), 1315-1317 (1985).
43. Gai S.A and Wittrup K.D. Yeast surface display for protein engineering and characterization. *Curr*. *Opin*. *Struct*. *Biol*. 17 (4), 467-473 (2007).
44. Mattheakis L.C., Bhatt R.R. and Dower W.J. An in vitro polysome display system for identifying ligands from very large peptide libraries. *Proc*. *Natl Acad*. *Sci*. *USA* 91 (19), 9022-9026 (1994).
45. Hanes J. and Pluckthun A. In vitro selection and evolution of functional proteins

using ribosome display. *Proc. Natl. Acad. Sci. USA* 94(10), 4937-4942 (1997).

46. Lungu O.I. et al. Designing photoswitchable peptides using the AsLOV2 domain. *Chem. Biol.* 19(4), 507-517 (2012).
47. Leaver-Fay A. et al. ROSETTA3: An object-oriented software suite for the simulation and design of macromolecules. *Methods Enzymol* 487, 545-574 (2011).
48. Speck J., Arndt K.M. and Müller K.M. Efficient phage display of intracellularly foldedproteins mediated by the TAT pathway. *Protein Eng. Des. Sel.* 24(6), 473-484 (2011).
49. Weiland, G. The enzyme-linked immunosorbent assay (ELISA)--a new serodiagnostic method for the detection of parasitic infections. *Munchener Medizinische Wochenschrift* 120 (44), 1457-1460 (1978).
50. Hui W. et al. LOVTRAP: an optogenetic system for photoinduced protein dissociation. *Nat. Methods* 13(9), 755-758 (2016).
51. Nord K. et al. Binding proteins selected from combinatorial libraries of an alpha-helical bacterial receptor domain. *Nat. Biotechnol.* 15, 772-777 (1997).
52. Kay C.W. et al. Blue light perception in plants-Detection and characterization of a light-induced neutral flavin radical in a C450A mutant of phototropin. *J. Biol. Chem.* 278,10973-10982 (2003).
53. Harper S.M., Christie J.M. and Gardner, K.H. Disruption of the LOV-Jα helix interaction activates phototropin kinase activity. *Biochemistry* 43, 16184-16192 (2004).
54. Schuster S.C. Next-generation sequencing transforms today's biology. *Nat. Methods* 5 (1), 16-18 (2008).
55. Sam B. and Patrick S.T. What is next generation sequencing? *Arch. Dis. Child. Educ. Pract. Ed.* 98(6), 236-238 (2013).
56. Van B.F., Holz J.B. and Revets H. The development of nanobodies for therapeutic applications. *Curr. Opin. Investig. Drugs* 10(11), 1212-1224 (2009).
57. Koide A. et al High-affinity single-domain binding proteins with a binary-code interface. *Proc. Natl. Acad. Sci. USA* 104(16), 6632-6637 (2007).
58. Binz H.K. et al. Designing repeat proteins: well-expressed, soluble and stable proteins from combinatorial libraries of consensus ankyrin repeat proteins. *J. Mol. Biol.* 332(2), 489-503 (2003).

59. Nygren P.A. Alternative binding proteins: Affibody binding proteins developed from a small three-helix bundle scaffold *FEBS J*. 275, 2668-2676 (2008).
60. Orlova A. et al. Tumor imaging using a picomolar affinity HER2 binding affibody molecule. *Cancer Res*. 66 (8), 4339-4348 (2006).
61. Renberg B. et al. Affibody molecules in protein capture microarrays: evaluation of multidomain ligands and different detection formats. *J. Proteome Res*. 6 (1), 171-179 (2007).
62. Tolmachev V. Radionuclide therapy of HER2-positive microxenografts using a 177Lu-labeled HER2-specific Affibody molecule. *Cancer Res*. 67 (6), 2773-2782 (2007).
63. Baker A.W. and Forest K.T. Action at a distance in a light receptor. *Nature* 509, 174-175 (2014).
64. Pathak G.P. et al. Benchmarking of Optical Dimerizer Systems. ACS Synth. Biol. 3(11), 832-838 (2014).
65. Steven C. Protein isoprenylation and methylation at carboxyl terminal-cysteine residues. *Annu. Rev. Biochem*. 61, 355-386 (1992).
66. Axelrod D. Total internal reflection fluorescence microscopy, *Method Cell Bio*. 30, 245-270 (1989).
67. Habuchi S. et al. mKikGR, a Monomeric Photoswitchable Fluorescent Protein. *PLoS One* 3(12), e3944 (2008).
68. Strack R. L. et al. A noncytotoxic DsRed variant for whole-cell labeling. *Nat. Methods* 5, 955-957 (2008).
69. Zhao Y. et al. An expanded palette of genetically encoded Ca^{2+} indicators. *Science* 33, 1888-1891 (2011).
70. Nagai T. et al. A variant of yellow fluorescent protein with fast and efficient maturation for cell-biological applications. *Nat. Biotechnol*. 20 (1), 87-90 (2002).
71. Tian L. et al. Imaging neural activity in worms, flies and mice with improved GCaMP calcium indicators. *Nat. Methods* 6, 875-881 (2009).
72. Kandel E. R. The molecular biology of memory: cAMP, PKA, CRE, CREB-1, CREB-2, and CPEB. *Mol. Brain* 5, 14-25 (2012).
73. Sassone-Corsi P. The cyclic AMP pathway. *Cold Spring Harbor Perspect. Biol*. 4, a011148 (2012).
74. Fan F. & Wood K. F. Bioluminescent assays for high-throughput screening.

Assay Drug Dev. Technol. 5, 127-136 (2007).

75. Anjia R. et al. Chromophore incorporation, P_r to P_{fr} kinetics, and P_{fr} thermal reversion of recombinant N-terminal fragments of Phytochrome A and B chromoproteins. *Biochemistry* 37, 9983-9990 (1998).
76. Leifer A. M. et al. Optogenetic manipulation of neural activity in freely moving *Caenorhabditis elegans*. *Nat. Methods* 8, 147-152 (2011).
77. Strickland D. et al. TULIPs: Tunable, light-controlled interacting protein tags for cell biology. *Nat. Methods* 9(4), 379-384 (2012).
78. Wagner J. R. et al. Mutational analysis of *Deinococcus radiodurans* bacteriophytochrome reveals key amino acids necessary for the photochromicity and proton exchange cycle of phytochromes. *J. Biol. Chem.* 283, 12212-12226 (2008).
79. Takala H. et al. signal amplification and transduction in phytochrome photosensors. *Nature* 509, 245-248 (2014).
80. Hanes J. and Pluckthun A. In vitro selection and evolution of functional proteins using ribosome display. *Proc. Natl. Acad. Sci. USA* 94(10), 4937-4942 (1997).
81. Yang X. et al. Temperature-scan cryocrystallography reveals reaction intermediates in bacteriophytochrome. *Nature* 479 (7373), 428-432 (2011).
82. Beckett D., Kovaleva E. and Schatz P.J. A minimal peptide substrate in biotin holoenzyme synthetase-catalyzed biotinylation. *Protein Sci.* 8(4), 921-929 (1999).
83. Fairhead M. and Howarth M. Site-specific biotinylation of purified proteins using BirA. *Methods Mol. Biol.* 1266, 171-184 (2015).
84. Ohashi H. et al. Efficient protein selection based on ribosome display system with purified components. *Biochem. Biophys. Res. Com.* 352, 270-276 (2007).
85. Shimizu Y. et al. Cell-free translation reconstituted with purified components. *Nat. Biotechnol.* 19, 751-755 (2001).
86. Devlin J.J., Panganiban L.C. and Devlin P.E. Random peptide libraries: a source of specific protein binding molecules. *Science* 249, 404-406 (1990).
87. Yang X., Kuk J. and Moffat K. Conformational differences between the Pfr and Pr states in Pseudomonas aeruginosa bacteriophytochrome. *Proc. Natl. Acad. Sci. USA* 106(37), 15639-15644 (2009).

88. Hook S.S. and Means A.R. Ca(2+)/CaM-dependent kinases: from activation to function. *Annu. Rev. Pharmacol. Toxicol.* 41, 471-505 (2001).
89. Burgie E.S. et al. Crystal Structure of Deinococcus Phytochrome in the photo-activated state reveals a cascade of Structural Rearrangements during Photo-conversion. *Structure* 24, 1-10 (2016).
90. Parks T.D. et al. Release of proteins and peptides from fusion proteins using a recombinant plant virus proteinase. *Anal. Biochem.* 216(2), 413-417 (1994).
91. Kapust R.B. et al. The P1' specificity of tobacco etch virus protease. *Biochem. Biophys. Res. Commun.* 294 (5), 949–55 (2002).
92. Rachel B.K. et al. Tobacco etch virus protease: mechanism of autolysis and rational design of stable mutants with wild-type catalytic proficiency. *Protein Engineering* 14(12), 993-1000 (2001).
93. Morrison K.L. and Weiss G.A. Combinatorial alanine-scanning. *Curr. Opin. Chem. Biol.* 5 (3), 302-307 (2001).
94. Shemiakina I.I. et al. A monomeric red fluorescent protein with low cytotoxicity. *Nat. Commun.* 3, 1204 (2012).
95. Yamanashi Y. et al. The yes-related cellular gene lyn encodeds a possible tyrosine kinase similar to p56lck. *Mol. Cell. Biol.* 7 (1), 237-243 (1987).
96. Wong J., Chen X. and Truong K. Engineering a temperature sensitive tobacco etch virus protease. *Protein Eng. Des. Sel.* 30(10), 705-712 (2017).
97. Wehr M.C. et al. Monitoring regulated protein-protein interactions using split TEV. *Nat. Methods* 3(12), 985-993 (2006).
98. Gray D.C., Mahrus S. and Wells J.A. Activation of specific apoptotic caspases with an engineered small-molecule-activated protease. *Cell* 142(4), 637-646 (2010).
99. Lee D. et al. A calcium- and light-gated switch to induce gene expression in activated neurons. *Nat. Biotechnol.* 35(9), 858-863 (2017).
100. Sun L. et al. Mixed lineage kinase domain-like protein mediates necrosis signaling downstream of RIP3 kinase. *Cell* 148 (1-2), 213-227 (2012).
101. Chen X. et al. Translocation of mixed lineage kinase domain-like protein to plasma membrane leads to necrotic cell death. *Cell Research* 24(1), 105-121 (2014).

102. Rekas A. et al. Crystal structure of venus, a yellow fluorescent protein with improved maturation and reduced environmental sensitivity. *J. Biol. Chem.* 277(52), 50573-50578 (2002).
103. Lecoeur H. Nuclear apoptosis detection by flow cytometry: influence of endogenous endonucleases. *Exp. Cell Res.* 277 (1), 1-14 (2002).
104. Gaforio J.J et al. Use of SYTOX green dye in the flow cytometric analysis of bacterial phagocytosis. *Cytometry* 48 (2), 93-96 (2002).
105. Allen J.E. and EI-Deiry E.S. Regulation of the human TRAIL gene. *Cancer Biol. Ther.* 13(12), 1143-1151 (2012).